International Journal of Mechanical, Industrial and Aerospace Sciences
ISSN: 2517-9950
Vol:14, No:9, 2020

Simulation and Design of an Aerospace Mission Powered by "Candy" Type Fuel Engines

N. Hernández Huertas, F. Rojas Mora

***Abstract*—**Sounding rockets are aerospace vehicles that were developed in the mid-20th century, and since then numerous investigations have been executed with the aim of innovate in this type of technology. However, the costs associated to the production of this type of technology are usually quite high, and therefore the challenge that exists today is to be able to reduce them. In this way, the main objective of this document is to present the design process of a Colombian aerospace mission capable to reach the thermosphere using low-cost "Candy" type solid fuel engines. This mission is the latest development of the Uniandes Aerospace Project (PUA for its Spanish acronym), which is an undergraduate and postgraduate research group at Universidad de los Andes (Bogotá, Colombia), dedicated to incurring in this type of technology. In this way, the investigations that have been carried out on Candy-type solid fuel, which is a compound of potassium nitrate and sorbitol, have allowed the production of engines powerful enough to reach space, and which represents a unique technological advance in Latin America and an important development in experimental rocketry. In this way, following the engineering iterative design methodology was possible to design a 2-stage sounding rocket with 1 solid fuel engine in each one, which was then simulated in RockSim V9.0 software and reached an apogee of approximately 150 km above sea level. Similarly, a speed equal to 5 Mach was obtained, which after performing a finite element analysis, it was shown that the rocket is strong enough to be able to withstand such speeds. Under these premises, it was demonstrated that it is possible to build a high-power aerospace mission at low cost, using Candy-type solid fuel engines. For this reason, the feasibility of carrying out similar missions clearly depends on the ability to replicate the engines in the best way, since as mentioned above, the design of the rocket is adequate to reach supersonic speeds and reach space. Consequently, with a team of at least 3 members, the mission can be obtained in less than 3 months. Therefore, when publishing this project, it is intended to be a reference for future research in this field and benefit the industry.

***Keywords*—**Aerospace missions, candy type solid propellant engines, design of solid rockets, experimental rocketry, low costs missions.

I. Introduction

THE competition over aerospace accelerated around the 1940s, when world powers such as the United States, Germany, England, and the Soviet Union wanted to demonstrate their military power by reaching the space [1]. Correspondingly, small rockets (sounding rockets) were designed, so they would reach space carrying some type of payload. Some of them were built, tested, and sometimes blown up, however the German-designed V-2 rocket (revenge weapon 2) was the first to cross the space barrier [2]. After this, governments decided to invest in this type of technology, giving way to large aerospace missions. Sputnik 1 (1957, Soviet Union) and Apollo 11 (1969, USA), among others, showed the great advances made in aerospace technologies during the 'space race', a period during which space exploration obtained an increasingly prominent place in the eyes of the world public. Thus, the consolidation of various aerospace research programs was initiated, such as the NASA Sounding Rocket Program Office. This program is responsible for providing orbital launch vehicles with support of field operations with the help of government agencies from different countries and is the most representative program in the field of research rocket [3]. In this way, missions have been carried out in 16 different places using sounding rockets [3], and it has been possible due to the ability to use high-powered, technologically developed solid fuels such as: ammonium perchlorate composite propellant (AP), hydroxyl-terminated polybutadiene (HTPB), among others. However, the use of this type of fuel in an aerospace mission represents a considerable increase in its costs, making it not feasible for many other projects in the world to execute an aerospace mission (a cost of about a million dollars per launch [4]).

In Table I, it is possible to appreciate the cost of building a solid-powered rocket engine. As can be seen from the table, building a solid fuel engine with suborbital height represents a high value in mission expenses. This is how it is observed that moving 1 kg of payload into space represents having a budget of more than 200 thousand USD (only for the construction of the engine), which makes it not feasible to carry out multiple projects.

TABLE I
Engine Cost (1st Stage in All Rockets Is a Hybrid Motor and All Other Stages Are SRM) [5]

Payload Mass	1st Stage Engine Cost	2nd Stage Engine Cost	3rd Stage Engine Cost	Total Engine Cost
200g	$679.720	$263.690	$79.930	$1.023.340
1kg	$634.090	$209.930	$86.860	$930.880
5kg	$1.138.700	$339.700	$80.900	$1.559.300

Importantly, in a solid fuel rocket, the propellant mass fraction is 96%, obtaining only the remaining 4% in the rocket [6]. This means that the costs associated with the production of rockets are strictly related to the use of fuel, which makes it possible to notice a significant reduction in expenses when obtaining lower priced and equally developed fuels.

"When making a rocket that is near 90% propellant (which

N. Hernandez Huertas is an undergraduate mechanical engineering student at Universidad De Los Andes (Bogota, Colombia) and active member of the PUA (phone: +573114642261; e-mail: cn.hernandez@uniandes.edu.co).

F. Rojas Mora is a Philosophy Doctor, MSc Mechanical Engineer, and an associate professor of the Mechanical Engineering Department of Universidad De Los Andes (Bogota, Colombia) (e-mail: farojas@uniandes.edu.co).

means it is only 10% rocket), small gains through engineering are literally worth more than their equivalent weight in gold" [6].

In order to be able to tackle the economic disadvantage faced by projects around the world regarding the expenses attributed to the use of AP/HTPB/AL fuels [5]; this research paper proposes using a low-cost Candy type solid propeller. While it is not a fuel that represents a high level of technological development, aided by recent advances in technology on the field of designing rockets and engines, this type of fuel could, theoretically, sustain a rocket reaching space. Consequently, the vehicle to be developed in this project will have characteristics similar to the "Improved Orion" developed by NASA, to reach heights of around 150 km above sea level, with the difference that a low-cost solid propeller is used [7]. In this way, this project plans to benefit the aerospace industry of many countries through this type of technology, resulting in a tangible improvement in the quality of life, as well as greater economic prosperity, health, and environmental quality, security, and protection [8].

II. Methodology

A. Engine Design

Solid fuel engines have a basic configuration, with essential elements to generate thrust. Fig. 1 shows the basic setup for a solid fuel engine.

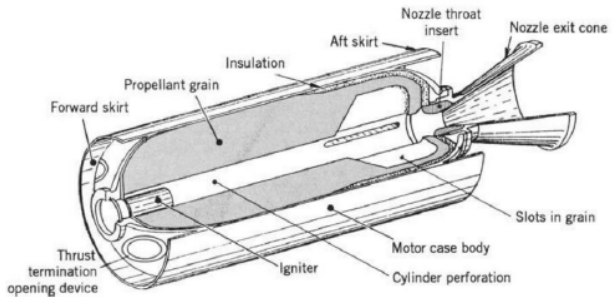

Fig. 1 Representation of a solid fuel engine [9]

Once knowing the components to be designed for the engine, it was followed the mathematical considerations and models in Sutton & Biblarz's book on Rocket Powered Elements [9]. In that order of ideas, "The principal assumption is the ideal rocket concept for facilities of mathematical relationships and the simplification of the equations. The rocket ideal concept describes a quasi-one-dimensional nozzle flow and the expansion exit flow in the nozzle is isentropic" [10]. Consequently, the principles and thermodynamic laws that would govern the mathematical model of the engine were determined. In that order of ideas, the following ones were mainly used [11]:

- Principle of conservation
- Principle of conservatism of mass
- Point of stagnation
- Perfect gas law
- Ratio of specific heats
- Isentropic flow process
- Mach number equation
- Momentum of thrust

Thus, using the previously numbered principles, a mathematical model was built in Microsoft Excel [12] software and the variables of interest in the construction of the engine were calculated (pressures, geometries, speeds, temperatures, and so on). On the other hand, it is important to highlight that the geometry of the propellant grain will determine the behavior of the motor over time. Specifically, this happens since the solid propulsion profile depends directly on the burning area, and likewise the burning rate depends directly on how the fuel is consumed within the combustion chamber. From the above, the developments and research carried out on solid propellant fuels (especially Candy) have allowed the generation of various representative curves of each geometry, and what guides guide in the development of this prototype [13]. With these previously designed considerations, an iterative design process of a "Candy" type solid fuel engine was started. In this sense, the "Illapa 1" engine that was built and tested on a test bench.

Fig. 2 PUA Illapa 1 Engine [10]

Fig. 3 Illapa 1 engine test and failure [10]

The first results of this engine allowed having an initial sketch of the behavior of this series of engines. In this sense,

as the engine failed to test it (Fig. 4), a failure analysis was performed which determined the technical specifications that the new engine design should have, so that it could be tuned on an aerospace mission. Thus, as a final step, a structural simulation of the engine was performed [14] with the new specifications concluded in the failure analysis (pressions, geometries, etc.), allowing the pertinent curves of the new "Candy" type solid fuel engine (Illapa 2 Engine) to be obtained, which will be presented in the results section. It is important to highlight that building and testing expenses of this engine were around of 2 thousand USD.

B. Fuselage

To design the rocket fuselage, it was suggested to use the iterative design method in engineering, based on graphs and tables found in the literature. In this way, the body of the rocket was molded using Fig. 4. As can be seen, the body finesses ratio of the rocket (length/diameter) should be kept between 8.5 and 10 so that the ratio of drag coefficients for pressure-skin is minimal. After this, the type of nose cone to be used in the rocket was selected, and therefore Fig. 5 was used. In such manner, when observing Fig. 5, and expecting that the movement should has a supersonic range, it was established that the rocket must have a Von Karman nose and therefore reduce the drag coefficient produced by this part. Equally, the dimensions of this part, the rocket nose, were set up by preserving a fineness ratio close to 3, which is justified with Fig. 6.

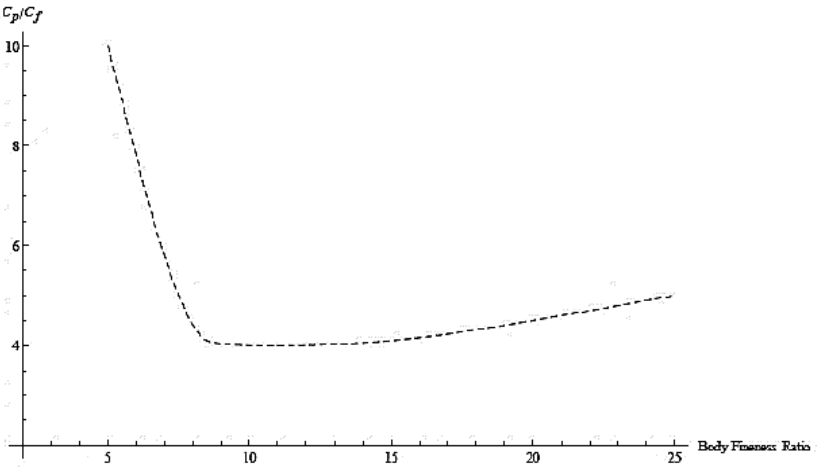

Fig. 4 Variation of drag coefficients with respect to body fineness ratio [15]

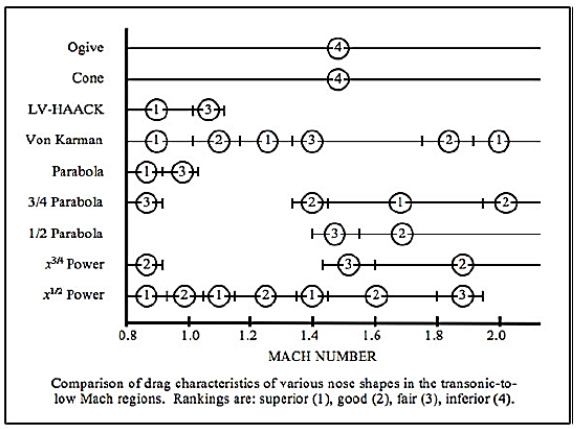

Fig. 5 Behavior of different types of nose cones under different Mach number [16]

Continuing with the rocket design, the geometry of the rocket fins was calculated. These elements are essential to achieve good stability in the rocket, since they allow having the center of pressure under the center of gravity, counteracting the generation of moments that can make the rocket rotate. In this sense, the recommendation of Stroick [18] was followed, which determines that for transonic regimes the trapezoidal fins have the best performance, while for supersonic regimes the "Tapered Swept" type fins are more suitable. Once this was obtained, the last element to design was the boattail. This element is essential to reduce drag coefficients, especially pressure, of the rocket. The design of this element was based on Fig. 7. As can be seen, the drag coefficients are lower when the boattail caliber is smaller, a criterion that had to be considered when designing the rocket.

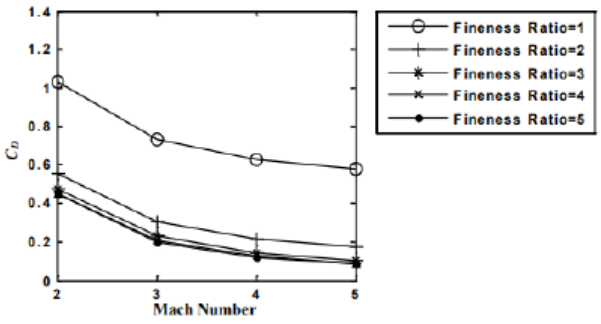

Fig. 6 Variation of drag coefficients with respect to nose cone fineness ratio [17]

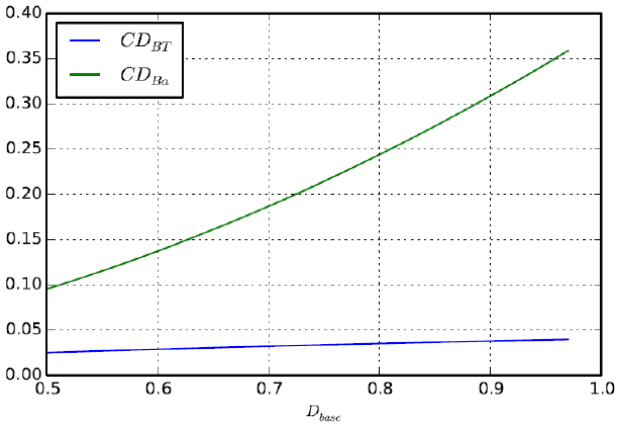

Fig. 7 Variation of drag coefficients with respect boattail caliber [19]

C. Flight Simulation

Under the parameters described above, the preliminary design of the rocket was built and simulated in the RockSim V9.0 ballistic movement software [20], since due to this modeler, the different variables that interest the project (altitude, range, Mach number, between others) can be calculated. Consequently, the simulation was carried out on the Gorgona Island located in the extreme west of the Republic of Colombia. The location of this island is far enough away from the civilian population, which means that it is safe to launch the rocket at this location. Table II represents the climatic conditions of the simulation.

TABLE II
LAUNCH SITE FEATURES FOR SIMULATION

GORGONA ISLAND	
Ocean	Pacific
Coordinates	2°58'17"N 78°11'04"O
Ground Distance	40 km from Guapi
RH	80%
Barometric Pressure	760 mm Hg
Height	0 m.a.s.l.
Population	Unhabituated

D. Computational Model

It is required to execute a finite element computational model in the vehicle since with this analysis it will be possible to calculate the stresses generated in the rocket as a result of the drag at such speed, as well as the pressure centers and the distribution of the streamlines. With the calculation of these variables it is expected to determine the feasibility of using the selected materials in the construction of the rocket, as well as the geometry designed for it. In this order of ideas, the finite element computational analysis was divided into 2, one related to fluid dynamics and another related to structural analysis. These analyzes were performed with the ANSYS computational tool. Consequently, the rocket was simulated based on NASA's wind tunnel tests of several of its rockets [21]. In these tests, the rockets are placed horizontally and anchored at their end, so that it is easier to observe and measure shock waves, flow streamlines, pressure distribution, among other things. The above described can be observed in greater detail in Fig. 8.

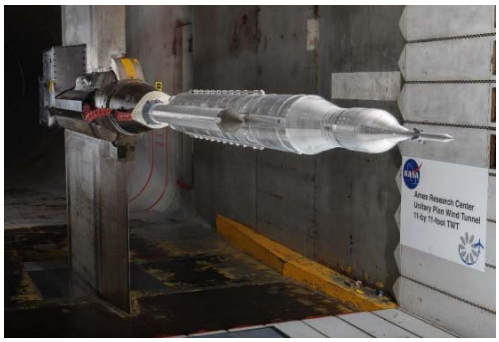

Fig. 8 Wind tunnel test of an SLS scale model at the Ames Research Center [22]

For the CFD analysis, the FLUENT tool of the aforementioned software (Ansys) was used. In this way, a turbulent air flow was simulated at the maximum speed shown in the RockSim simulations, in the direction of the rocket, starting from the nose, with a turbulence intensity of 15%. A limit was placed upstream and downstream of the body at a distance of approximately 3 times its height. In addition, a lateral distance of approximately 5 times its diameter was located (as would happen in a wind tunnel test) [23]. With this it can be possible to fully observe the streamlines and shock waves through the device. On the other hand, the mesh was of the hybrid type, this means that the mesh is made up of prismatic elements in the viscous region located very close to the body, while the tetrahedral elements were used to fill the remaining fluid. Thus, one size of each element can be selected enough for the convergent system in a single solution. Likewise, to perform the structural analysis of the rocket, the Static Structural tool of the aforementioned software was used. In that order of ideas, a communication channel was built between the Fluent tool and the Static Structural, so that the loads on the rocket were those generated by the air flow. This analysis is of vital importance when designing aerospace vehicles. The engineer Piatak, stated that:

> "A structural dynamic analysis will predict the response of the launch vehicle due to dynamic events such as liftoff, buffet, wind gusts at high altitudes, staging, and engine start up and shut down. It is an important process for ensuring a safe flight for not only the launch vehicle but also any payload that it carries to orbit" [22].

In this way, a conventional mesh was carried out with a refinement in the sections that presented high pressures in the CFD analysis, in order to have a system that converged to a single solution.

III. RESULTS

After building and testing the "Candy" type solid propulsion engines (Illapa 2 Engines), Figs. 9 and 10 were obtained (each figure constitutes the thrust curve during the combustion

time). Likewise, Tables III and IV, which represent the dimensions and the performance of the engine, can be appreciated.

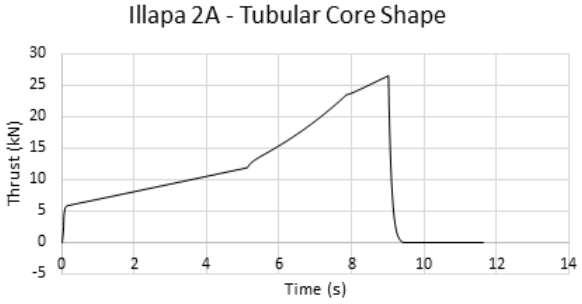

Fig. 9 Thrust vs time solid propellant motor Illapa 2A [14]

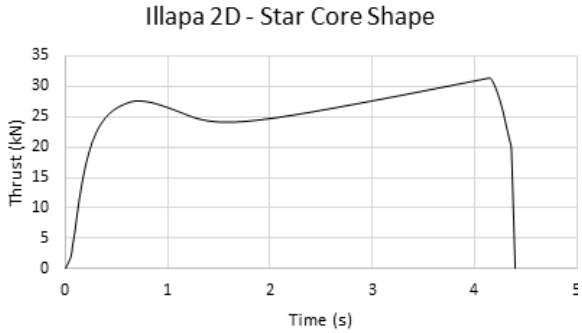

Fig. 10 Thrust vs time solid propellant motor Illapa 2D [14]

TABLE III
ILLAPA 2A ENGINE DIMENSION TABLE AND PERFORMANCE SUMMARY [14]

PARAMETER	VALUE
Combustion chamber diameter	254 mm
Outer diameter of the grain	235 mm
Inner diameter of the grain	80 mm
Combustion chamber length	1600 mm
Grain length	250 mm
Maximum thrust	26420,663 N
Total Impulse	156329.01 N s
Specific Impulse	158.41 s
Burning time	12.77 seconds

TABLE IV
ILLAPA 2D ENGINE DIMENSION TABLE AND PERFORMANCE SUMMARY [14]

PARAMETER	VALOR
Combustion chamber diameter	254 mm
Outer diameter of the grain	235 mm
Inner diameter of the grain	100 mm
Combustion chamber length	1600 mm
Grain length	250 mm
Grain outlet diameter	135 mm
Fin with	30 mm
Number of fins in the grain	8
Maximum thrust	30345.756 N
Total impulse	90596.46 N s
Specific Impulse	81.16 s
Burning time	15.96 seconds

As can be seen in Fig. 9, the Illapa 2A motor has a straight-line behavior and more burning time. This is ideal for the first stage since in order to generate movement and overcome inertia, a progressive change in motor impulse is required. On the other hand, by observing the Illapa 2D motor curves, thrust behaves constantly, so this is ideal for the second stage since at this point the rocket needs to continue to propel itself steadily and for a longer period. On the other hand, knowing that the Illapa series engines were going to be used, the rocket was designed following the previously evidenced methodology. The sketch of the vehicle can be seen in Fig. 11, as well as the summary of its main characteristics.

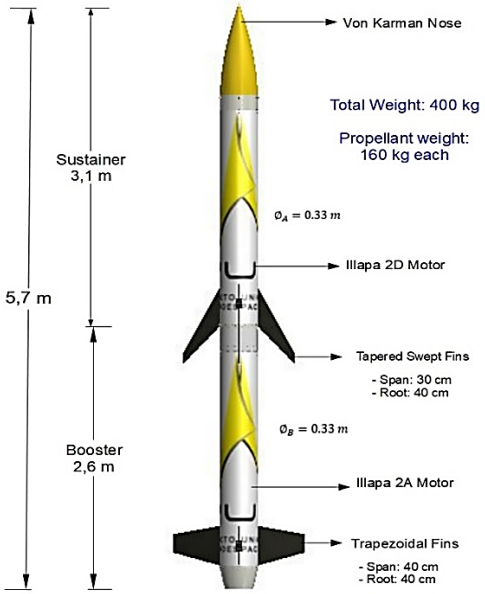

Fig. 11 Dimensions and main characteristics of the rocket

Once the rocket design was obtained, the ballistic movement simulation was performed, the results can be seen in Figs. 12 and 13.

As it can be seen in Fig. 12, the apogee of the rocket (using the Illapa 2A and 2D engines, with a payload of 2 kg) is approximately 150 km above sea level. In addition to this, an adequate variation of the Mach number (which is related to the speed) can be seen, since this value begins to increase when the engines are started. Once the combustion stage ends, a considerable decrease in the speed of the vehicle is observed, which leads to the rocket reaching its peak and beginning to descend. At that time, an increase in the speed of the device is observed again as a result of the acceleration generated by the gravitational force on it, which then decreases due to the use of parachutes. Finally, it can be seen that the vehicle's fall range is approximately 60 km above the launch site, an aspect that must be considered in the logistics of the mission. On the other hand, the values of the drag force of the rocket during its ballistic movement can be observed in Fig. 13. In this order of ideas, it can be seen that, at the moment of combustion of the engines, the value of the drag force increases considerably, as a result of the increase in the speed of the device. However,

after this stage ends, the drag force has minimum values, which demonstrates the good aerodynamic design of the rocket. Finally, at the end of the graph, an increase in this force can be observed since at this point is where the rocket parachutes are deployed, which must use the energy of the wind to decrease the speed of the vehicle's fall. With these results in mind, having a maximum speed of approximately 1700 m/s, the computational model (CFD and structural analysis) was performed. As can be seen, the flow velocity is distributed almost evenly throughout the rocket. However, there are points where the speed can increase considerably, such as the second stage fuselage in the regions just behind the fins. This means that, in this region, the speed manages to increase its magnitude as a result of the wake generated by the fin and some type of vorticity generated in this region. Likewise, it can be seen the detachment of the boundary layer and the wake generated by the rocket when it is in motion. For its part, the stream lines show normal behavior in the trajectory of the rocket and for that reason it can be established that the rocket has a geometry sufficiently aerodynamic to have minimum drag force values, which is reflected in the graphs of the simulations in the RockSim. Moreover, the pressure contour shows that there is a greater concentration at the tip of the nose, in the contact of the fins and at the exit of the boattail. In other words, the incident air flow on these surfaces generates an increase in pressure as a result of the friction force of the air against them, which are key points for structural analysis. Finally, Figs. 16-18 indicate the results achieved in the structural analysis.

As it could be observed in Figs. 16-18 the rocket is strong enough to carry out the ballistic mission. That is, by observing the state of equivalent stresses, it can be determined that, although the rocket is subjected to high loads, it is strong enough to withstand them. Specifically, in the stress state an average of approximately 900 MPa can be appreciated, which includes considerations of normal (mostly bending) and shear (mostly torsional) stresses, which influence the deformation of each part. On the other hand, Fig. 17 shows that the nose suffers a high deformation rate as a result of the increase in temperature on its surface and by the shock waves generated by the air. However, when observing Fig. 18 (the safety factor of the rocket), it can be determined that this region is sufficiently safe and secure since the value of this factor is approximately 15. Similarly, it can be seen that in some regions (close to the boattail), the safety factor decreases to almost 10 and even in some cases it can reach values close to 5. However, as previously explained, for this structural analysis the rocket was anchored in a similar way to the wind tunnel, that is, horizontally and held at the end. This means that in the regions close to this support, higher load values are generated, giving way to greater compression, tension, torsion, shear and bending stresses. However, in reality this situation is not considered, since the rocket is free at this end and therefore fluctuations in loads and moments do not occur, therefore, the safety factor of these parts can increase considerably, making the rocket safe for the mission.

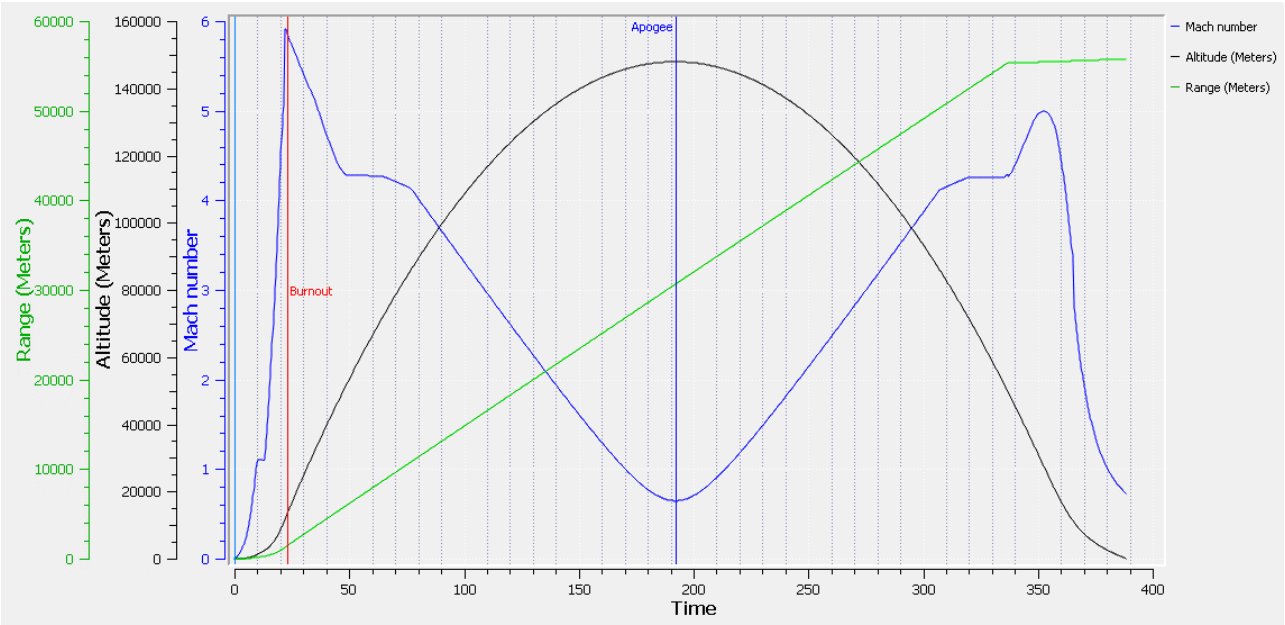

Fig. 12 Variation of the altitude, fall range and Mach number of the vehicle throughout the flight time [20]

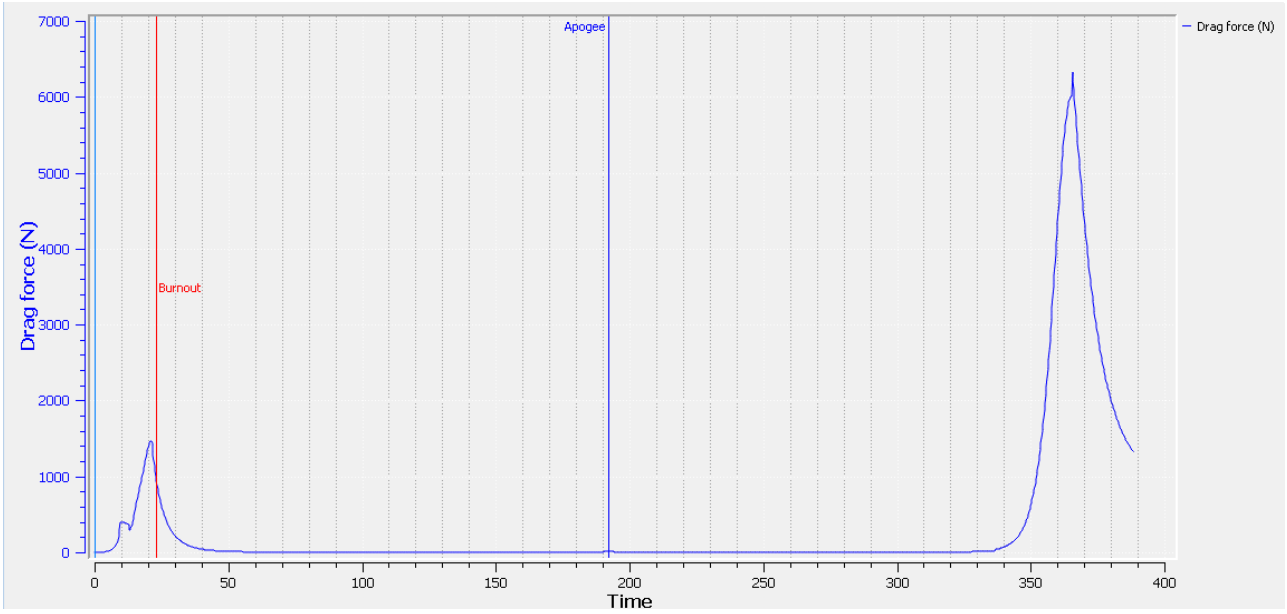

Fig. 13 Variation of the drag force of the vehicle throughout the flight time [20]

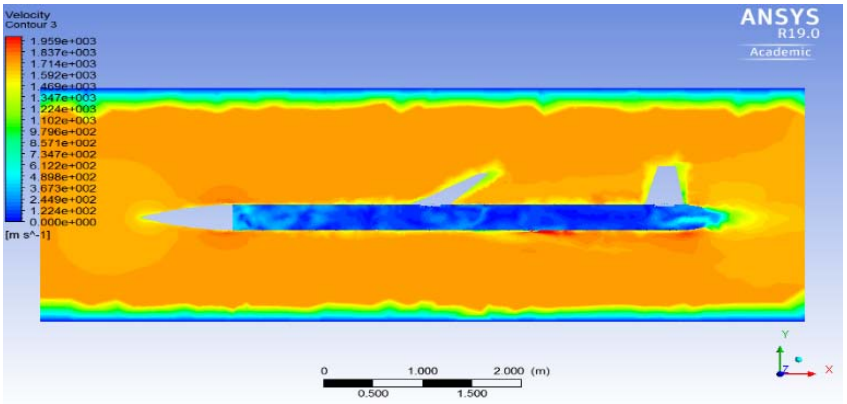

Fig. 14 Velocity contour of the rocket at Mach 6

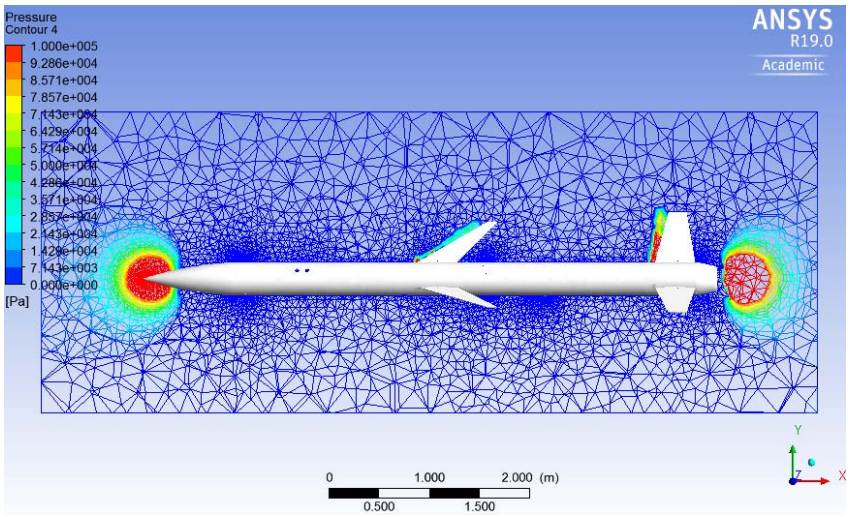

Fig. 15 Pressure contour of the rocket at Mach 6

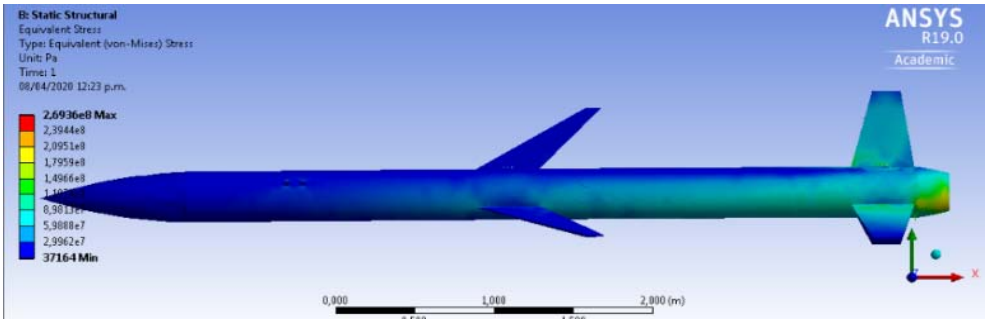

Fig. 16 Equivalent stress of the rocket at Mach 6

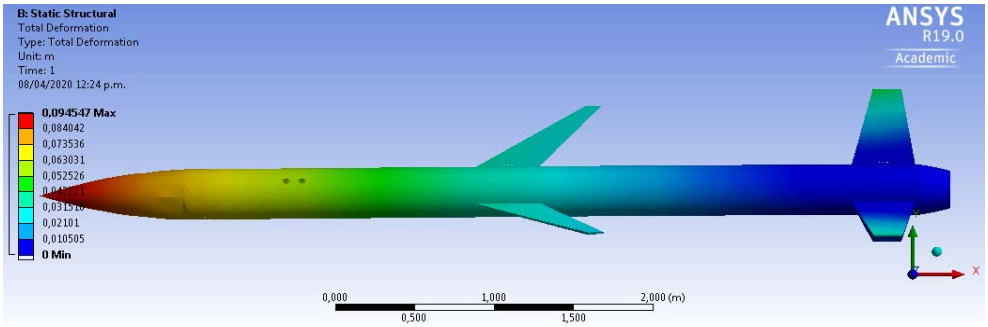

Fig. 17 Total deformation of the rocket at Mach 6

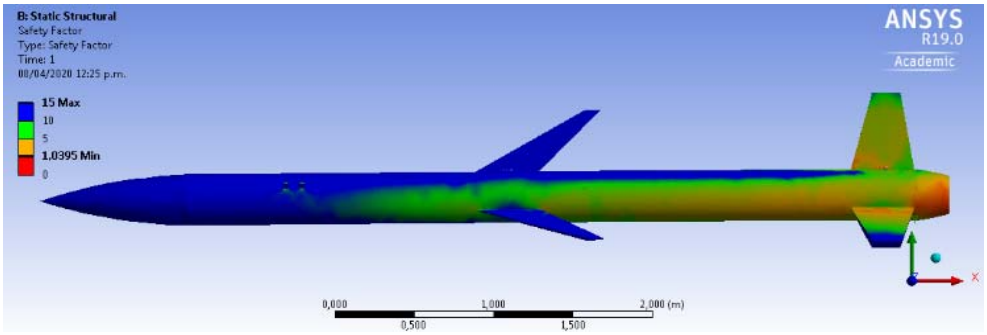

Fig. 18 Safety factor of the rocket at Mach 6

IV. Conclusions

By executing this project, it was determined that, through an iterative process, it is possible to design a rocket intended to reach space heights with the help of low-cost, high-power, candy-type solid fuel engines. For this reason, replicating this mission will largely depend on the ability to produce candy-type engines as powerful as those designed in this project. Consequently, the fulfillment of this mission represents a significant advance in the aerospace industry and in the history of experimental rocketry. In this way, it is feasible to propose projects in the aerospace framework that impact the technological and social progress of different countries and, therefore, the contribution to future research. With this in mind, the next step is to physically construct the launch pad and the rocket to launch it, since there is enough theoretical, experimental, and computational evidence for a successful mission.

References

[1] C. Cook, The Aerospace Industry: Its History and How it Affects the U.S. Economy, Yale-New Haven Teachers Institute, 2014.
[2] NASA, "La evolucion del cohete" 12 2001. (Online). Available: https://pwg.gsfc.nasa.gov/stargaze/Mrockhis.htm.
[3] NASA, "NASA Sounding Rocket Program Overview," Dr. Robert F. Pfaff, 11 10 2019. (Online). Available: https://rscience.gsfc.nasa.gov/index.html.
[4] B. Dorminey, "Sounding Rockets Still Astronomy's Unsung Workhorses," Forbes, 06 2013. (Online). Available: www.forbes.com/sites/brucedorminey/2013/06/30/sounding-rockets-still-astronomys-unsung-workhorses/#2a944b265985.
[5] S. Bluestone, "Project Bellerophon," University of Purdue, 2008.
[6] NASA, "The Tyranny of the Rocket Equation," 2012. (Online). Available: www.nasa.gov/mission_pages/station/expeditions/expedition30/tryanny.html#backtoTop.
[7] B. Bland, "Sounding Rocket Program Office," NASA, 2020. (Online). Available: https://sites.wff.nasa.gov/code810/about.html.
[8] W. H. Gerstenmaier, Interviewee, Centro de Comunicaciones de la Red del Espacio Profundo (DSN). (Interview). 09 2015.
[9] G. Sutton and O. Biblarz, Rocket Propulsion Elements, Wiley-

lnterscience Publication, 2000.
[10] M. Simahan, "Design, Construction and Testing of a solid propellant engine," Universidad De Los Andes, 2017.
[11] R. Nakka, «Solid Rocket Motor Theory,» 07 2001. (En línea). Available: https://www.nakka-rocketry.net/rtheory.html. (Último acceso: 2020).
[12] C. Galarza y F. Rojas, «Design of a candy propellant rocket motor by a computer aided system and its performance in static testing» Universidad de los Andes, Bogota, 2015.
[13] R. Nakka, "Solid Rocket Motor Theory -- Propellant Grain," 05 07 2001. (Online). Available: https://www.nakka-rocketry.net/th_grain.html.
[14] D. Romero, "Diseño, Construcción y Pruebas de un Sistema de Propulsión a Combustible Sólido con Motores Illapa- 2 de 30kN de Empuje para Misiones Suborbitales," Universidad De Los Andes, Bogota D.C., 2019.
[15] M. Mendenhall, "Tactical missile aerodynamics," American Institute of Aeronautics and Astronautics, Prediction methodology, 1992.
[16] D. Hoover, "Ten pounds to ten thousand feets: Designing an inexpensive and reusable rocket," American Institute of Aeronautics and Astronautics, 2009.
[17] A. Saw and A. Mahdi Al-Obaidi, "Drag of Conical Nose at Supersonic Speeds," 04 2013. (Online). Available: https://university2.taylors.edu.my/EURECA/2014/downloads/35.pdf.
[18] G. Stroick and T. Minnesesota, Nose Cone & Fin Optimization, Off We Go Rocketry, 2011.
[19] G. Ciodaro, "Construccion y ensamble del fuselaje para el vehiculo AINKAA," Universidad De Los Andes, 2014.
[20] Apogee Rockets, "RockSim V9.0 Software," 2019. (Online). Available: https://www.apogeerockets.com/RockSim/RockSim_Information.
[21] NASA, "Wind Tunnel Testing Used to Understand the Unsteady Side of Aerodynamics," 3 11 2013. (Online). Available: https://www.nasa.gov/exploration/systems/sls/sls-aerodynamics.html.
[22] NASA, "SLS Model 'Flies' Through Langley Wind Tunnel Testing," 28 11 2012. (Online). Available: https://www.nasa.gov/exploration/systems/sls/sls_windtunnel.html.
[23] S. Kilikevičius, A. Fedaravičius, A. Survila and L. Patašienė, "Analysis of Aerodynamic Characteristics of the Rocket-Target for the „Stinger" System," 2015.